On 3D retrieval from photos

Tarik Filali Ansary, Jean-Philippe Vandeborre, Mohamed Daoudi

▶ **To cite this version:**

Tarik Filali Ansary, Jean-Philippe Vandeborre, Mohamed Daoudi. On 3D retrieval from photos. 3rd IEEE International Symposium on 3D Data Processing, Visualization and Transmission (3DPVT'06), Jun 2006, Chapel Hill, North Carolina, United States. hal-00725580

HAL Id: hal-00725580
https://hal.science/hal-00725580

Submitted on 27 Aug 2012

HAL is a multi-disciplinary open access archive for the deposit and dissemination of scientific research documents, whether they are published or not. The documents may come from teaching and research institutions in France or abroad, or from public or private research centers.

L'archive ouverte pluridisciplinaire **HAL**, est destinée au dépôt et à la diffusion de documents scientifiques de niveau recherche, publiés ou non, émanant des établissements d'enseignement et de recherche français ou étrangers, des laboratoires publics ou privés.

On 3D retrieval from photos

Tarik Filali Ansary, Jean-Phillipe Vandeborre, Mohamed Daoudi
FOX-MIIRE Research Group (LIFL UMR 8022 CNRS/USTL)
(GET/INT – Telecom Lille 1)
email: {filali, vandeborre, daoudi}@enic.fr
http://www-rech.enic.fr/fox-miire

Abstract

In this paper, we propose a method for 3D-model retrieval from one or more photos. This method provides an "optimal" selection of 2D views to represent a 3D-model, and a probabilistic Bayesian method for 3D-model retrieval from realistic photos and sketches using these views. The characteristic view selection algorithm is based on an adaptive clustering algorithm and uses statistical model distribution scores to select the optimal number of views. We also introduce a Bayesian approach to score the probability of correspondence between the queries and the 3D-models. We present our results on the *Princeton 3D Shape Benchmark database* (1814 3D-models) and 50 photos (real photographs, sketches, synthesised images). A practical on-line 3D-model retrieval system based on our approach is available on the web to asset our results [1].

1. Introduction

The development of 3D modelling and digitalising technologies has made the 3D-model generation process much easier. Also, through the Internet, users can download a large number of free 3D-models from all over the world. This has increased the need for developing efficient techniques for content-based 3D-model retrieval.
Recently, some experimental 3D Shape search engines have been made, such as the 3D-model search engine at *Princeton University* [2], the 3D model retrieval system at *The National Taiwan University* [3], the Ogden IV system at *The national Institute of Multimedia Education*, Japan [4], the 3D retrieval engine at *Utrecht University* [5] and the 3D model similarity search engine at *The University of Konstanze* [6].
To search a database for 3D-models that are visually similar to a view, a sketch or a photo of a 3D-model is a very intuitive way. But, it is a challenging problem. The main idea in 3D retrieval using 2D-views or photos is that two 3D-models are similar if they also look similar from different angles. So, the proposed solutions are to correspond one or more photos (sketches, views) to the 3D-models they are similar to.
Funkhouser et al. [2] apply view-based similarity to implement a 2D sketch query interface. In the preprocessing stage, a descriptor of a 3D-model is obtained by 13 thumbnail images of boundary contours as seen from 13 view directions.
Chen et al. [3] use 100 orthogonal projections of an object and encode them by Zernike moments and Fourier descriptors. The running time of the retrieval process is reduced by a clever multi-step approach supporting early rejection of non-relevant models.
Using aspect graphs, Cyr and Kimia [7] specify a query by a view of 3D-objects. A descriptor of a 3D-model consists of a set of views. The number of views is kept small by views clustering and by representing each cluster by one view, which is described by a shock graph. Schiffenbauer [8] presents a complete survey of aspect graphs methods.
Using shock matching, Macrine et al. [9] apply indexing using topological signature vectors to implement view-based similarity matching more efficiently.
Filali et al. [10] propose an nearest neighbour-like framework to choose the characteristic views of a 3D-model. Some early experiments were made on CAD models retrieval from photos but was only applied on a small database.
However, to our knowledge no on-line 3D-model search engine can retrieve 3D-models from one or more photos. A complete survey on 3D shape retrieval can be found in Tangelder and Veltkamp [11].
In this paper, we propose a method for 3D-model retrieval from one or more photos(photographs, sketch, views) based on 2D views. This method aims at providing an optimal selection of 2D views from a 3D-model, and a probabilistic Bayesian method for 3D-model indexing from these views.
This paper is organised as follows. In section 2, we present the main principles of our method for characteristic view selection. In section 3, our probabilistic 3D-model retrieval from photos is presented. Then, the results obtained from a database of 50 images and 1814 3D-models (Princeton 3D Shape Benchmark database) are discussed demonstrat-

ing the performance of our method. Finally, we present our on-line 3D search engine.

2 Selection of characteristic views

Let $D_b = \{M_1, M_2, \ldots, M_N\}$ be a collection of N three-dimensional models. We want to represent each 3D-model M_i by a set of 2D views that best represent it. To achieve this goal, we first generate an initial set of views from the 3D-model, then we reduce this set to only those that best characterise this 3D-model. In this paragraph, we present our algorithm for characteristic view selection from a three-dimensional model.

2.1 Generating the initial set of views

To generate the initial set of views for a model M_i of the collection, we create 2D views (projections) from multiple viewpoints. These viewpoints are equally spaced on the unit sphere. In our current implementation, we use 320 initial views. The views are silhouettes only, which enhance the efficiency and the robustness of the image metric. To represent each of these 2D views, we use 49 coefficients of Zernike moment descriptor [12]. Due to the use of Zernike moments, the approach is robust against translation, rotation, and scaling.

2.2 Characteristic views selection

As every 2D view is represented by 49 Zernike moment coefficients, choosing a set of characteristic views that best characterise the 3D-models (320 views) is equivalent to choose a subset of points that represent a set of 320 points in a 49-dimension space. Choosing X characteristic views which best represent a set of $N = 320$ views is well known as a *clustering problem*.

One of the widely used algorithm in clustering is *K-means* [13] algorithm. Its attractiveness lies in its simplicity and in its local-minimum convergence properties. However, it has one main shortcoming: the number of clusters K has to be supplied by the user.

As we want from our method to adapt the number of characteristic views to the geometrical complexity of the 3D-model, we use a method derived from K-means. Instead of using a fixed number of clusters, we propose to use a range in which we will choose the "optimal" number of clusters. In our case, the range will be $[1, \ldots, 40]$. In this paper, we assume that the maximum number of characteristic views is 40. This number of views is a good compromise between speed, descriptor size and representation (section 4).

We proceed now to demonstrate how to select the characteristic view set and also how to select the best K within the given range. In essence, the algorithm starts with one characteristic view (K equal to 1), we add characteristic views where they are needed, and we do a global K-means on the data starting with characteristic views as cluster centers. We continue alternating between adding characteristic views and doing a global K-means until the upper bound for characteristic view number (40) is reached. During this process, for each K, we save the characteristic view set.

To add new characteristic views, we use the idea presented in the X-means clustering method by Dan Pelleg [14]. First, for every cluster of views represented by a characteristic view (Figure 1(a)), we select two views that have the maximum distance in this cluster (Figure 1(b)). Next, in each cluster of views, we run a local K-means (with $K = 2$) for each pair of selected views.

By *local*, we mean that only the views that are in the cluster are used in this local clustering (Figure 1). Note that Figure 1 and 2 are just a schematic example, as we represent a view in a two dimensional space. In our system each view is represented by a vector in a 49 dimensional space (corresponding to the 49 Zernike moment features extracted from the view).

At this point, a question arises: "Are the two new characteristic views giving more information on the region than the original characteristic view?" To answer this question, we use Bayesian Information Criteria (BIC) [15], which scores how likely the representation model (using one or two characteristic views) fits the data.

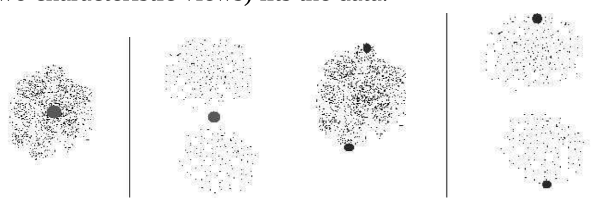

(a) (b)

Figure 1: Local K-means on each part of the views clusters with $K = 2$.

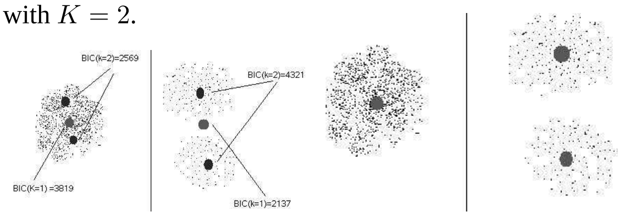

(a) (b)

Figure 2: Selecting the representations (with 1 or 2 characteristic views) that have the higher BIC score.

According to the outcome of the test, the model with the highest score is selected (Figure 2). These clusters of the views which are not represented well by the current centroids will receive more attention by increasing the number of centroids in them.

We continue alternating between global K-means and local K-means on clusters belonged to the characteristic views until the upper bound for the characteristic view number is reached. Then, we compare the BIC score of each characteristic view set. Finally, the best characteristic view set will be the one that gets the highest BIC score on all the views.

3 Probabilistic approach for 3D indexing

The main idea of our probabilistic approach is that **not** all views of a 3D-model have the same importance. There are views which represent the 3D-model better than others. On the other hand, simple objects (e.g. cube, sphere) can be at the root of more complex objects, so they have a bigger probability to be relevant. In this section, we present a probabilistic approach that takes into account that views do not have the same importance, and that simple objects have higher probability to appear than more complex one.

Each model of the collection D_b is represented by a set of characteristic views $V = \{V_1, V_2, \ldots, V_C\}$, with C the number of characteristic views. To each characteristic view corresponds a set of represented views called V_r.

As mentioned before, we want to find the 3D models that corresponds to one or more request photos. We assume that in a query $Q = \{I_1, I_2, \ldots, I_K\}$ all K the images represent the same object. Considering a query Q, we wish to find the model $M_i \in D_b$ which is the closest to the query Q. This model is the one that has the highest probability $P(M_i/Q)$. Knowing that a query is composed of one or more images, $P(M_i/Q)$ can be written:

$$P(M_i|Q) = \sum_{k=1}^{K} \frac{1}{K} P(M_i|I_k),$$

With K the number of images in the query Q. Let H be the set of all the possible hypotheses of correspondence between the request image I_k and a model M_i, $H = \{h_1^k \vee h_2^k \vee \ldots \vee h_N^k\}$. A hypothesis h_p^k means that the view p of the model is the request image I_k. The sign $\vee$ represents *logic or operator*. Let us note that if an hypothesis h_p^k is true, all the other hypotheses are false. $P(M_i|I_k)$ can be expressed by $P(M_i|H^k)$. We have:

$$P(M_i|H^k) = \sum_{j=1}^{N} P(M_i, V_{M_i}^j|h_j^k).$$

The sum $\sum_{j=1}^{N} P(M_i, V_{M_i}^j|h_j^k)$ can be reduced to the only true hypothesis $P(M_i, V_{M_i}^j|H_j^k)$. In fact, an image from the request Q can match only one characteristic view from the model M_i . We choose the characteristic view with the maximum probability.

$$P(M_i|Q) = \sum_{k=1}^{K} \frac{1}{K} Max_j(P(M_i, V_{M_i}^j|h_j^k)) \tag{1}$$

Using the Bayes theorem, we have:

$$P(M_i, V_{M_i}^j|h_j^k) = \frac{P(h_j^k, V_{M_i}^j|M_i)P(M_i)}{P(h_j^k)}. \tag{2}$$

On the other hand, we have:

$$P(h_j^k, V_{M_i}^j|M_i) = P(h_j^k|V_{M_i}^j, M_i)P(V_{M_i}^j|M_i), \tag{3}$$

and,

$$P(h_j^k) = \sum_{i=1}^{N} \sum_{j=1}^{\hat{v}} P(h_j^k|V_{M_i}^j, M_i)P(V_{M_i}^j|M_i)P(M_i)). \tag{4}$$

By using (1), (2), and (3) we obtain:

$$P(M_i, V_{M_i}^j|h_j^k) = \tag{5}$$

$$\frac{P(h_j^k|V_{M_i}^j, M_i)P(V_{M_i}^j|M_i)P(M_i)}{\sum_{i=1}^{N} \sum_{j=1}^{\hat{v}} P(h_j^k|V_{M_i}^j, M_i)P(V_{M_i}^j|M_i)P(M_i)}.$$

Finally:

$$P(M_i|Q) = \sum_{k=1}^{K} \frac{1}{K} \tag{6}$$

$$Max_j(\frac{P(h_j^k|V_{M_i}^j, M_i)P(V_{M_i}^j|M_i)P(M_i)}{\sum_{i=1}^{N} \sum_{j=1}^{\hat{v}} P(h_j^k|V_{M_i}^j, M_i)P(V_{M_i}^j|M_i)P(M_i)}).$$

As mentioned before, not all three-dimensional models in the collection have the same probability to occur. Our algorithm assumes that the simpler is the three-dimensional model, the smaller is the number of the characteristic views. To model the fact that the larger the relative number of views of a model M_i, the smaller the probability of the model, we estimate $P(M_i)$, the probability to observe a three-dimensional model M_i by:

$$P(M_i) = \frac{e^{(-\alpha N(V_{M_i})/N(V))}}{\sum_{i=1}^{N} e^{(-\alpha N(V_{M_i})/N(V))}}, \tag{7}$$

where $N(V_{M_i})$ is the number of characteristic views of the model M_i, $N(V)$ is the total number of characteristic views for the set of the models of the collection D_b. α is a coefficient that reduces the effect of small values of the exponential in $P(M_i)$.

On the other hand, there are views that contain more information than other ones. We assume that the greater the number of represented views $N(Vr_{M_i}^j)$ for a characteristic view $V_{M_i}^j$, the more this characteristic view is important and the more information it contains about the three-dimensional model. So, we modelled $P(V_{M_i}^j|M_i)$ the probability to observe the characteristic view j of the model M_i by:

$$P(V_{M_i}^j|M_i) = \frac{1 - \beta e^{(-\beta N(Vr_{M_i}^j)/N(Vr_{M_i}))}}{\sum_{j=1}^{\hat{v}} (1 - \beta e^{(-\beta N(Vr_{M_i}^j)/N(Vr_{M_i}))})}, \tag{8}$$

where $N(Vr^j_{M_i})$ is the number of views represented by the characteristic view j of the model M, $N(Vr_{M_i})$ is the total number of views represented by the model M_i. The β coefficient is introduced to reduce the effect of small values of the view probability. We use the values $\alpha = \beta = 1/100$ which give the best results during our experiments.

The value $P(h^k_j|V^j_{M_i}, M_i)$ is the probability that, knowing that we observe the characteristic view j of the model M_i, this view corresponds to image k of the request Q:

$$P(h^k_j|V^j_{M_i}, M_i) = \frac{e^{-D(I_k, V^j_{M_i})}}{\sum_{j=1}^{\hat{v}} e^{-D(I_k, V^j_{M_i})}}, \tag{9}$$

where $D(I_k, V^j_{M_i})$ is the Euclidean distance between the Zernike descriptors of the image k of the request model Q and $V^j_{M_i}$ is the characteristic view j of the three-dimensional model M_i.

To summarise, in this section we presented our Bayesian retrieval framework which takes into account the number of characteristic views of the model and the importance (amount of information) of its views.

4 Experimental results

In this section, we present the experimental process and the results we obtained. The algorithms we described in the previous sections have been implemented using C++ and the TGS Open-Inventor libraries. The system consists of an off-line characteristic view extraction algorithm and an on-line retrieval process.

In our method, each model was normalised for size by isotropically rescaling it so that the average Euclidean distance from points on its surface to the center of mass is 0.5. Then, all models were normalised for translation by moving their center of mass to the origin.

In the off-line process, the characteristic view selection takes about 18 seconds per model on a PC with a Pentium IV 2.4 GHZ CPU. In the on-line process, the comparison takes less than 1 second for 1814 3D-models.

To evaluate our method, we used the *Princeton Shape Benchmark database* (PSB), a standard shape benchmark widely used in shape retrieval community. *Princeton Shape Benchmark* (PSB) appeared in 2004 and is one of the most exhaustive benchmarks for 3D shape retrieval. It contains a database of 1814 classified 3D-models collected from 293 different Web domains. There are many classifications given to the objects in the database. During our experiments we used the finest granularity classification, composed of 161 classes. Most classes contain objects with a particular function (e.g cars). Yet, there are also cases where objects with the same function are partitioned in different classes based on their shapes (e.g, round tables versus rectangular tables) [16].

The mean number of views for the *Princeton Shape Benchmark database* is 23 views per model. The mean size for a 3D model descriptor is 1,113 bytes.

To evaluate the algorithms we presented on the previous sections, we selected 50 images from the Internet. The images correspond to 10 classes of the *Princeton Shape Benchmark* (five images per class): Airplanes, Bicycles, Chairs, Dogs, Guns, Hammers, Humans arms out, Helicopters, Pots and Swords. The images are composed of six sketches, six synthetized images and 38 real photos of different sizes.

As the request photos will be compared to the characteristic views of the 3D models, a pre-processing stage is needed. The extraction of the Zernike moments of characteristic views and querry images is as follows:

1. Transform input image to grey scale image.

2. Get edge image from the grey level image using the *Canny filter* [17] and binarize it, the object is composed of the edge pixels.

3. Normalise the binarized edge image to accomplish object scale invariance.

4. Move the origin of the image to the centroid of the object, obtain object translation invariance.

5. The extracted Zernike features start from the second order moments. We extract up to the twelfth order Zernike moments corresponding to 49 features.

Figure 3: Two queries and their corresponding edge images.

Figure 3 shows two images from the query-image database and their corresponding edge images. As the reader may have noticed, in the experiments we use images with a simple background. This problem can be partially solved using a more sophisticated segmentation algorithm, but this is beyond the scope of this paper.

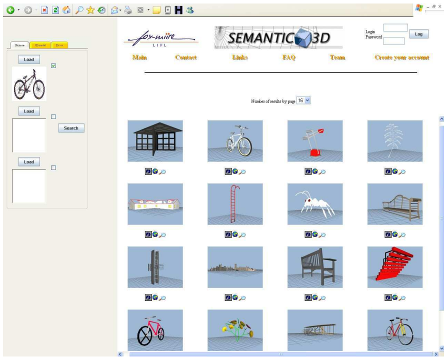

Figure 4: 3D retrieval results using one photo.

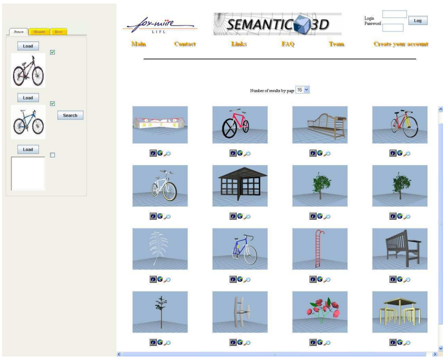

Figure 5: 3D retrieval results using two photos.

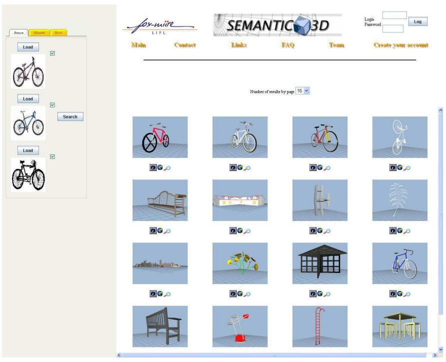

Figure 6: 3D retrieval results using three photos.

Figures 4, 5 and 6 show the results of a query using respectively, one, two and three images of a bicycle. The left side of the figures represent the queries and the right side represent the 16 top retrieved 3D-models. Figure 4 shows the sixteen first result of a query using one photo from the 1814 3D-models in the database. From the seven 3D-models representing a bicycle in the database, three are in the fifteen top retrieved 3D-models. This number raises to four out of seven when we use two images (Figure 5). Using three images (Figure 6)we retrieved five out of seven in the top sixteen retrieved 3D-models.

To evaluate the performance of our method we used Recall VS. Precision curves. Recall VS. Precision curves are well known in the literature of content-based search and retrieval. The recall and precision are defined as follow:

$$\text{Recall} = N/Q, \text{Precision} = N/A,$$

where N is the number of relevant models retrieved in the top A retrievals, Q is the number of relevant models in the collection, which is the number of models to which the query belongs to.

For each of the 10 image classes, we present five different Recall VS. Precision Curves :

- **Using 1 image:** This curve represents the mean Recall VS. Precision curve for 5 queries using one image from the image-class.
- **Using 2 images:** This curve represents the mean Recall VS. Precision curve for 5 queries using two random images from the image-class.
- **Using 3 images:** This curve represents the mean Recall VS. Precision curve for 5 queries using three random images from the image-class.
- **Using 4 images:** This curve represents the mean Recall VS. Precision curve for 5 queries using four random images from the image-class.
- **Using 5 images:** The Recall VS. Precision curve using the five images of the class.

Figures 7 to 16 show the Recall Vs Precision plots for the ten image-classes. We can notice that using more images in a request results in better precision's rates.

In Figures 9,10,11, the precision gain is 26% using two images instead of one. The gain can be up to 75% using 4 images instead of one as shown in Figure 15. Overall, our method works quite well on hand-drawing, synthetized images(or 3D model views) and photos.

The gain from using multiple images in a query face the problem of "how to get this query images?" Using web images search-engines, camera or hand-drawing can solve the problem, but it is still time and effort consuming to get or draw five or more images.

We believe that using two or three photos makes a good compromise between time-effort and accuracy.

Our work can be applied to e-shopping or CAD models retrieval from photos, where instead of browsing big catalogues of products user present one or more photos of a similar object and the search engine will return the most relevant results.

To experiment our algorithms and to asset the results presented in the previous sections, we developed an on-line 3D search engine. Our search engine can be reached from any device having compatible web browser (PC, PDA, SmartPhone, etc.) [1].

Depending on the web access device he/she is using, the user face two different kind of web interfaces : a rich web interface for full-featured web browsers, and a simpler interface for PDA web browsers. In both cases, the results returned by the 3D search engine are the same. The only difference lies in the design of the results presentation. The 3D database available for tests of our 3D search engine is the *Princeton Shape Benchmark Database* [16].

5 Conclusion

In this paper, we propose a 3D-model retrieval from photos based on characteristic view similarity. We also propose a characteristic view selection algorithm that relates the number of views to its geometrical complexity. The number of characteristic views varies from 1 to 40. We also propose a new probabilistic retrieval approach that corresponds one or more photos representing the same object to 3D models characteristic views. The experiments of our method on *Princeton Shape Benchmark Database* (1814 3D-models), show the good retrieval results using one or more photos. Using Recall VS Precision plots, we present our result on 10 different image-classes. The precision gain from using more than one photo can be up to 78%. Our work can be applied to e-shopping or CAD models retrieval from photos, where instead of browsing big catalogues of products, the user presents one or more photos of a similar object and the search engine will return the most relevant results. A practical 3D-model retrieval system based on our approach is available on the Web for on-line tests [1].To our knowledge, it is the first 3D retrieval system from photos on line.

References

[1] "Fox-miire 3d retrieval system," http://www-rech.enic.fr/3dretrieval.

[2] T. Funkhouser, P. Min, M. Kazhdan, A. Haderman, D. Dobkin, and D. Jacobs, "A search engine for 3D models," *ACM Transactions on Graphics*, vol. 22, no. 1, pp. 83–105, 2003.

[3] D. Y. Chen, X. P. Tian, Y. T. Shen, and M. Ouhyoung, "On visual similarity based 3D model retrieval," in *Eurographics*, 2003, vol. 22, pp. 223–232.

[4] M. T. Suziki, "A search engine for polygonal models to support development of. 3d e-learning applications," in *In The Tenth International World Wide Web Conference Poster Proceedings*, 2001, pp. 182–183.

[5] J. W.H. Tangelder and R. C. Veltkamp, "Polyhedral model retrieval using weighted point sets," in *International Conference on Shape Modeling and Applications*, 2003, pp. 119–131.

[6] D. V. Vranic, "An improvement of rotation invariant 3D shape descriptor based on functions on concentric spheres," in *IEEE International Conference on Image Processing*, 2003, pp. 757–760.

[7] C. M. Cyr and B. Kimia, "3D object recognition using shape similarity-based aspect graph," in *IEEE International Conference on Computer Vision*, 2001, pp. 254–261.

[8] R. D. Schiffenbauer, "A survey of aspect graphs," Tech. Rep. TR-CIS-2001-01, CIS, 2001.

[9] D. Macrini, A. Shokoufandeh, S. Dickenson, K. Siddiqi, and S.Zucker, "View based 3-D object recognition using shock graphs," in *IEEE International Conference on Pattern Recognition*, 2002, vol. 3, pp. 24–28.

[10] T. Filali Ansary, J. P. Vandeborre, and M. Daoudi, "A framework for 3D CAD models retrieval from 2D images," *Annals of Telecommunications, special issue on Technologies and tools for 3D imaging*, vol. 60, no. 11-12, pp. 1337–1359, November-December 2005.

[11] J. W. H. Tangelder and R. C. Veltkamp, "A survey of content-based 3D shape retrieval methods," in *IEEE Shape Modeling International*, 2004, pp. 145–156.

[12] A. Khotanzad and Y. H. Hong, "Invariant image recognition by Zernike moments," *IEEE Transactions on Pattern Analysis and Machine Intelligence*, vol. 12, no. 5, pp. 489–497, May 1990.

[13] R. O. Duda and P. E. Hart, "Pattern classification and scene analysis," *John Wiley and Sons*, 1973.

[14] D. Pelleg and A. Moore, "X-means: Extending k-means with efficient estimation of the number of clusters," in *International Conference on Machine Learning*, 2000, pp. 727–734.

[15] G. Schwarz, "Estimating the dimension of a model," *The Annals of Statistics*, vol. 6, pp. 461–464, 1978.

[16] "Princeton shape benchmark," 2004, http://shape.cs.princeton.edu/benchmark.

[17] J. F. Canny, "A computational approach to edge detection," *IEEE Trans. Pattern Analysis and Machine Intelligence*, vol. 8, no. 6, pp. 679–698, 1986.

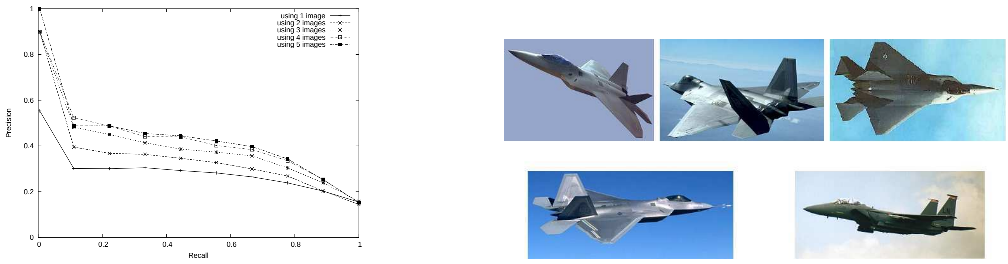

Figure 7: RP plots and request pictures for airplanes class.

Figure 8: RP plots and request pictures for bicycles class.

Figure 9: RP plots and request pictures for chairs class.

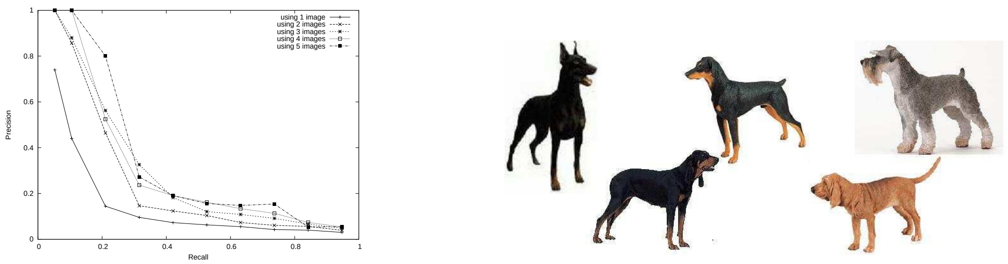

Figure 10: RP plots and request pictures for dogs class.

Figure 11: RP plots and request pictures for guns class.

Figure 12: RP plots and request pictures for hammers class.

Figure 13: RP plots and request pictures for humans class.

Figure 14: RP plots and request pictures for helicopters class.

Figure 15: RP plots and request pictures for pots class.

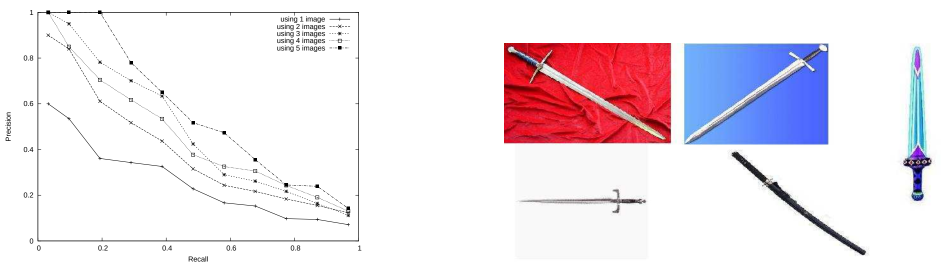

Figure 16: RP plots and request pictures for swords class.